

# ELECTROMAGNETIC DESIGN OF THE PROTOTYPE SPOKE CAVITY FOR THE JAEA-ADS LINAC

J. Tamura\*, Y. Kondo, B. Yee-Rendon, S. Meigo, F. Maekawa, K. Hasegawa, JAEA, Ibaraki, Japan  
E. Kako, K. Umemori, H. Sakai, T. Konomi, KEK, Ibaraki, Japan

## Abstract

The Japan Atomic Energy Agency (JAEA) is proposing an accelerator-driven subcritical system (ADS) as a future project to transmute long-lived nuclides to short-lived or stable ones. In the JAEA-ADS, a high-power proton beam of 30 MW with a final beam energy of 1.5 GeV is required with a high reliability. Furthermore, the accelerator needs to be operated in a continuous wave mode in order to be compatible with the reactor operation. As the first step toward the detailed design of the JAEA-ADS linac, we are planning to demonstrate a high-field measurement by prototyping a low-beta single spoke resonator (SSR1). We performed the electromagnetic design, and confirmed that the cavity performances of the SSR1 model with and without dimensional constraint.

## INTRODUCTION

The Japan Atomic Energy Agency (JAEA) is proposing an accelerator-driven subcritical system (ADS) as a future project to transmute long-lived nuclides to short-lived or stable ones. In the JAEA-ADS, a high-power proton beam of 30 MW with a final beam energy of 1.5 GeV is required with a high reliability. Furthermore, the accelerator needs to be operated in a continuous wave (CW) mode in order to be compatible with the reactor operation. Since a normal conducting (NC) structure raises a difficulty in cavity cooling under the CW operation, a superconducting (SC) linac would be a suitable solution. In the proposed linac, the high-intensity proton beam is accelerated by an NC radio-frequency quadrupole (RFQ) and low-beta SC cavities such as a half-wave resonator (HWR) and a single spoke resonator (SSR), and finally accelerated to the designed beam energy of 1.5 GeV by elliptical cavities. Figure 1 shows the layout of the accelerating structure of the JAEA-ADS linac. Although the cavity's beta and transition energy of each cavity type are currently under review, this accelerating structure is similar to that proposed in [1].

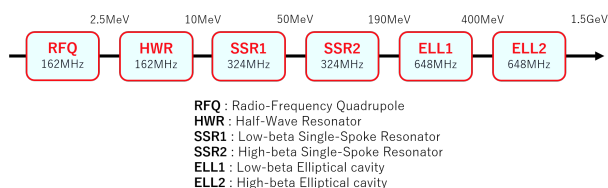


Figure 1: Accelerating structure of the JAEA-ADS linac.

\* jtamura@post.j-parc.jp

As the first step toward the detailed design of the JAEA-ADS linac [2–4], we are planning to demonstrate a high-field measurement by prototyping a low-beta single spoke resonator (SSR1) which operating frequency is 324 MHz. This study will provide us various insights about developing a SC  $\lambda/2$  structure of which we have almost no experience. Moreover, it will also enable us to acquire valuable information such as how much accelerating gradient is achievable with required stability. In this paper, preliminary result of the electromagnetic design of the prototype spoke cavity is presented.

## CAVITY BETA OF PROTOTYPE SSR1

We set the geometrical beta:  $\beta_g$  of the prototype SSR1 to 0.188, since the transit time factor stay high in the energy region where the SSR1 is supposed to be used. Assuming a sinusoidal field distribution along the beam axis (the origin:  $z = 0$  means the center of 2-cell  $\pi$ -mode cavity),

$$E_z(z) = \sin\left(\frac{2\pi}{\beta_g \lambda} z\right) \quad (1)$$

where  $\lambda$  is the resonant wavelength, the transit time factor can be expressed by the following formula.

$$T(\beta) = \frac{\int E_z(z) \sin(2\pi z/\beta\lambda) dz}{\int |E_z(z)| dz} \quad (2)$$

$$= \frac{\pi}{4} \left( \frac{\sin\left(2\left(\frac{\beta_g}{\beta} - 1\right)\frac{\pi}{2}\right)}{2\left(\frac{\beta_g}{\beta} - 1\right)\frac{\pi}{2}} - \frac{\sin\left(2\left(\frac{\beta_g}{\beta} + 1\right)\frac{\pi}{2}\right)}{2\left(\frac{\beta_g}{\beta} + 1\right)\frac{\pi}{2}} \right) \quad (3)$$

As shown by the blue dot in Fig. 2, the transit time factor with  $\beta_g = 0.188$  have its maximum value of 0.818

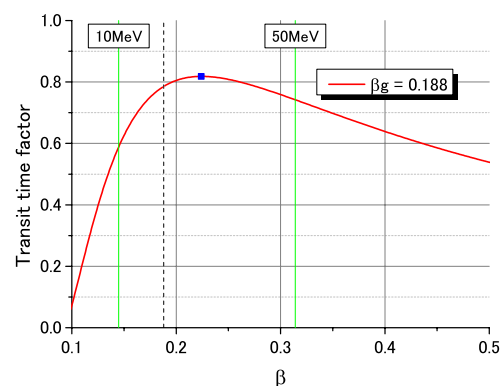


Figure 2: Transit time factor of 2-cell  $\pi$ -mode structure with  $\beta_g = 0.188$ .

Content from this work may be used under the terms of the CC BY 3.0 licence (© 2019). Any distribution of this work must maintain attribution to the author(s), title of the work, publisher, and DOI.

at  $\beta = 0.224$ . We call this beta as optimal beta:  $\beta_{\text{opt}}$  ( $T_{\text{max}} = T(\beta_{\text{opt}}) = T(0.224) = 0.818$ ).

We fixed the interval of two accelerating gaps of the prototype SSR1 to  $\beta_g \lambda/2 = 87.0$  mm. This is invariable even in the optimization of cavity dimension such as the gap length.

## PROTOTYPE SSR1

We had to impose a dimensional constraint to the prototype SSR1 so that the cavity can be put in the existing cryostat for high-field measurement. We restricted the diameter of the outer conductor (the cavity height) no larger than 380 mm. Therefore, the cavity length was increased to adjust the cavity frequency to the operating one of 324 MHz, whereas the cavity height is optimized for the frequency adjustment in case of general  $\lambda/2$  cavities. This constraint made the cavity longitudinally large. Consequently, the shunt impedance per length of the cavity was decreased.

We performed the electromagnetic design of the prototype SSR1 with the dimensional constraint. The design model was simulated by using CST Microwave Studio. Figure 3 shows the design model of the prototype SSR1. One can see from Fig. 3 that the length of the end drift-tube (re-entrant nose) is so long in contradistinction to that of the accelerating gap.

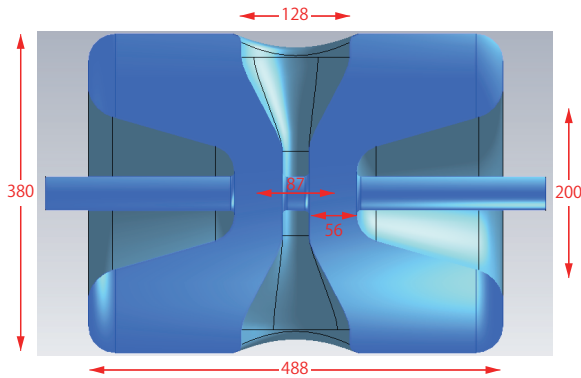


Figure 3: Design model of the prototype SSR1. The cavity dimensions are described by millimetric unit.

We defined the accelerating voltage:  $V_{\text{acc}}$  with particle (proton) velocity of  $\beta = \beta_{\text{opt}} = 0.224$ . Therefore,  $V_{\text{acc}}$  is expressed as

$$V_{\text{acc}} = V_0 T(\beta_{\text{opt}}) = \int E_z(z) \sin\left(\frac{2\pi}{\beta_{\text{opt}}\lambda} z\right) dz \quad (4)$$

where  $V_0$  is an axial RF voltage:  $V_0 \equiv \int |E_z(z)| dz$ . In Fig. 4, the distribution of  $E_z(z)$  and  $E_z(z) \times \sin(2\pi z/\beta_{\text{opt}}\lambda)$  are shown by black and red line, respectively. As for the accelerating gradient, we defined  $E_{\text{acc}}$  by dividing the accelerating voltage by the effective length:  $L_{\text{eff}} = 2 \times (\beta_{\text{opt}}\lambda/2) = 207.3$  mm as  $E_{\text{acc}} = V_{\text{acc}}/L_{\text{eff}}$  [5].

The design model of was optimized for better cavity performance as follows:

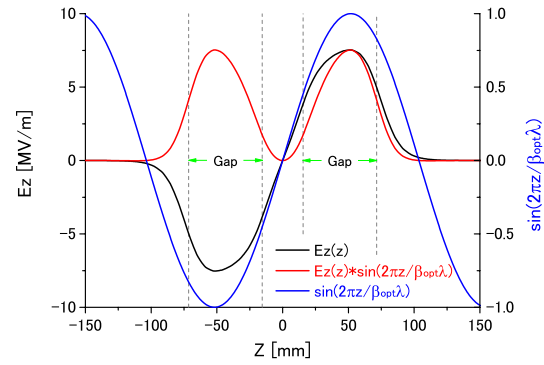


Figure 4: Accelerating field along the beam axis obtained by the simulation. The field strength is normalized to have the cavity's stored energy of 1 Joule.

- higher geometrical factor:  $G = Q_0 R_s$ , where  $Q_0$  and  $R_s$  are unloaded  $Q$  factor and surface resistance, respectively.
- higher  $R$  over  $Q$ :  $R/Q = V_{\text{acc}}^2/\omega W$ , where  $\omega$  and  $W$  are angular frequency and stored energy, respectively.
- lower peak electric field ratio:  $E_{pk}/E_{\text{acc}}$ .
- lower peak magnetic field ratio:  $B_{pk}/E_{\text{acc}}$ .

The surface electric and magnetic field of the simulated prototype SSR1 is shown in Fig. 5. The electric peak field is located in the re-entrant nose tip. On the other hand, the magnetic peak field is located around the taper part of the spoke electrode.

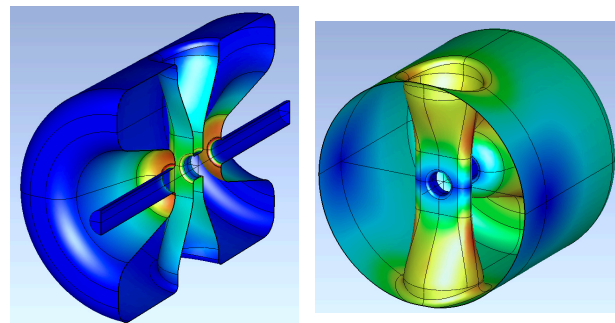


Figure 5: Surface electric (left) and magnetic (right) field of the designed prototype SSR1.

The dimensional parameters of the cavity were optimized by following the standard procedure [6]. Representative examples of the dimensional optimization of the prototype SSR1 are shown in Fig. 6. The figures of merit of the op-

Table 1: Performance Parameters of the Prototype SSR1

Figures of merit	Unit	
$G$	95	Ohm
$R/Q$	261	Ohm
$E_{pk}/E_{\text{acc}}$	4.23	
$B_{pk}/E_{\text{acc}}$	4.67	mT/(MV/m)

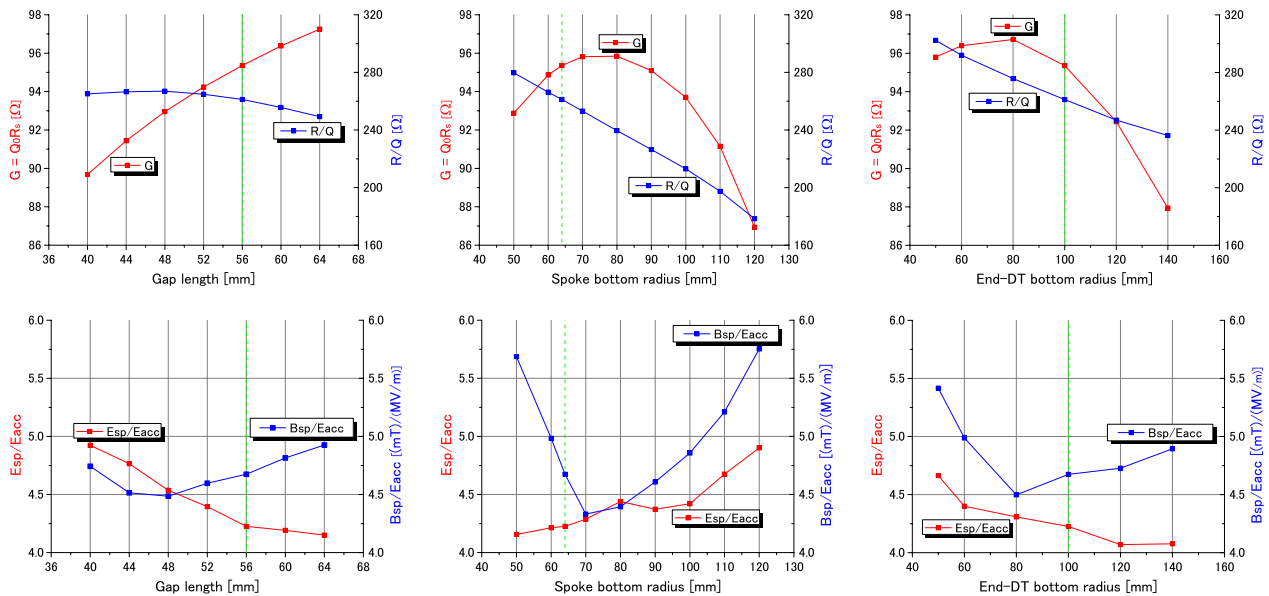


Figure 6: Representative examples of the dimensional optimization of the prototype SSR1. Left: Gap length. Center: Spoke bottom radius (radius of the inner conductor base). Right: End-DT bottom radius (radius of the end drift-tube base).

timized prototype SSR1 are listed in Table 1. These are not very different from that of a modern spoke cavity [7–9]. The notable characteristic is comparatively small  $B_{pk}/E_{acc}$  ratio. The reason could be considered that the increased volume, where the magnetic field distribute, decreased the peak magnetic field under the same stored energy.

### SSR1 WITHOUT CONSTRAINT

To investigate the cavity performance parameters, we designed the SSR1 which does not have dimensional constraint we put to the prototype SSR1. The designed SSR1 with fixed cavity length of 300 mm is shown in Fig. 7. Figure 8 shows the surface electric and magnetic field of the simulated SSR1 without constraint. The locations of the

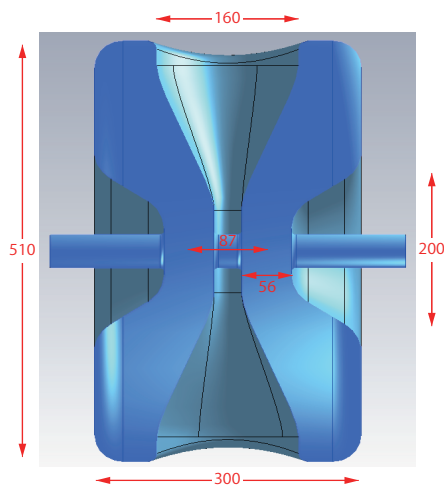


Figure 7: Design model of the SSR1 without constraint. The cavity dimensions are described by millimetric unit.

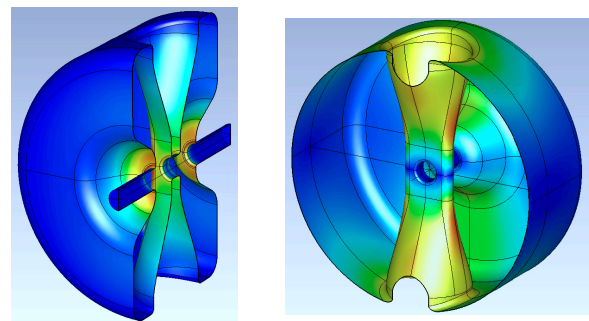


Figure 8: Surface electric (left) and magnetic (right) field of the designed SSR1 without constraint.

peak fields are same as the case of the prototype SSR1. The figures of merit of the optimized SSR1 without constraint are listed in Table 2. Comparing the figures of merits listed in Table 1 and 2, we could confirm that the cavity performance of the prototype SSR1 is not so degraded from that of the SSR1 without constraint.

Table 2: Performance Parameters of the SSR1 without Constraint

Figures of merit	Unit	
$G$	90	Ohm
$R/Q$	235	Ohm
$E_{pk}/E_{acc}$	3.81	
$B_{pk}/E_{acc}$	6.22	mT/(MV/m)

## SUMMARY

We performed the electromagnetic design of the SSR1. To put the cavity in the existing cryostat for high-field measurement, we had to impose a dimensional constraint to the prototype SSR1. By comparing the figures of merit of the designed prototype SSR1 with that of the designed SSR1 without constraint, we found that these cavity performances are comparable. We continue to proceed further investigation for the prototype SSR1 and prepare for its manufacturing.

## REFERENCES

- [1] B. Mustapha, S. V. Kutsaev, J. A. Nolen, and P. N. Ostroumov, "A Compact Linac Design for an Accelerator Driven System", in *Proc. 27th Linear Accelerator Conf. (LINAC'14)*, Geneva, Switzerland, Aug.-Sep. 2014, paper MOPP003, pp. 52–54.
- [2] B. Yee-Rendon, Y. Kondo, F. Maekawa, S. Meigo, and J. Tamura, "Beam Optics Design of the Superconducting Region of the JAEA ADS", in *Proc. 10th Int. Particle Accelerator Conf. (IPAC'19)*, Melbourne, Australia, May 2019, paper MOPGW040, pp. 181-183.
- [3] B. Yee-Rendon, Y. Kondo, F. Maekawa, S. Meigo, and J. Tamura, "Electromagnetic Design of the Low Beta Cavities for the JAEA ADS", in *Proc. 10th Int. Particle Accelerator Conf. (IPAC'19)*, Melbourne, Australia, May 2019, paper WEPRB028, pp. 2870-2872.
- [4] B. Yee-Rendon, Y. Kondo, F. Maekawa, S. Meigo, and J. Tamura, "Design of the Elliptical Superconducting Cavities for the JAEA ADS", in *Proc. 10th Int. Particle Accelerator Conf. (IPAC'19)*, Melbourne, Australia, May 2019, paper WEPRB029, pp. 2873-2876.
- [5] A. Facco, "Tutorial on Low Beta Cavity Design", in *Proc. 12th Int. Conf. RF Superconductivity (SRF'05)*, Ithaca, NY, USA, Jul. 2005, paper SUA04, pp. 21–33.
- [6] B. Mustapha, Z. A. Conway, A. Kolomiets, and P. N. Ostroumov, "Electromagnetic Design Optimization of a Half-Wave Resonator", in *Proc. 15th Int. Conf. RF Superconductivity (SRF'11)*, Chicago, IL, USA, Jul. 2011, paper MOPO044, pp. 192–196.
- [7] L. Ristori *et al.*, "Design, Fabrication and Testing of Single Spoke Resonators at Fermilab", in *Proc. 14th Int. Conf. RF Superconductivity (SRF'09)*, Berlin, Germany, Sep. 2009, paper THPPO011, pp. 550–554.
- [8] L. Ristori *et al.*, "Design of Single Spoke Resonators for Project X", in *Proc. 15th Int. Conf. RF Superconductivity (SRF'11)*, Chicago, IL, USA, Jul. 2011, paper MOPO024, pp. 122–126.
- [9] L. Ristori *et al.*, "Development and Performance of 325 MHz Single Spoke Resonators for Project X", in *Proc. 16th Int. Conf. RF Superconductivity (SRF'13)*, Paris, France, Sep. 2013, paper FRIOB02, pp. 1187–1192.